Editorial Manager(tm) for Acta Physiologiae Plantarum
Manuscript Draft

Manuscript Number:

Title: Biochemical characterization of the Arabidopsis KS-type dehydrin protein, whose gene expression is constitutively abundant rather than stress dependent

Article Type: Original Research

Corresponding Author: Masakazu Hara

Corresponding Author's Institution:

First Author: Masakazu Hara

Order of Authors: Masakazu Hara;Yuri Shinoda;Masayuki Kubo;Daiju Kashima;Ikuo Takahashi;Takanari Kato;Tokumasa Horiike;Toru Kuboi

Abstract: Dehydrins are known as plant stress-responsive genes. Arabidopsis thaliana has 10 dehydrin genes. Among them, one of the highly expressed genes is a KS-type dehydrin (At1g54410). However, the gene product, which is a histidine-rich dehydrin whose molecular mass is 11 kDa (AtHIRD11), has not been studied. Thus, we report the biochemical characterization of the AtHIRD11 protein. Although the AtHIRD11 protein was detected in all organs of Arabidopsis, the bolting stem and the flower showed higher accumulation than the other organs, with the AtHIRD11 protein detected in the cambial zone of the stem vasculature. Most of the AtHIRD11 protein was found to be a bound form. The bound AtHIRD11 was solubilized by 1 M NaCl solution. The extracted AtHIRD11 was retained in immobilized metal-affinity chromatography, and eluted by an imidazole gradient. The native AtHIRD11 prepared from Arabidopsis was partially phosphorylated, but further phosphorylated by casein kinase 2 in vitro. Metal-binding assays indicated that Zn2+ may be the best metal for AtHIRD11 binding. These results suggest that AtHIRD11 is a metal-binding dehydrin that shows a house-keeping expression in Arabidopsis.

Title

Biochemical characterization of the *Arabidopsis* KS-type dehydrin protein, whose gene expression is constitutively abundant rather than stress dependent

Authors

Masakazu Hara[a]*, Yuri Shinoda[a], Masayuki Kubo[a], Daiju Kashima[a], Ikuo Takahashi[a], Takanari Kato[a], Tokumasa Horiike[b], Toru Kuboi[a]

[a]Faculty of Agriculture, Shizuoka University,
836 Ohya, Suruga-ku, Shizuoka,
422-8529, Japan

[b]Division of Global Research Leaders, Shizuoka University,
836 Ohya, Suruga-ku, Shizuoka,
422-8529, Japan

*Corresponding author

Name and address for editorial correspondence

Masakazu Hara
Faculty of Agriculture, Shizuoka University,
836 Ohya, Suruga-ku, Shizuoka,
422-8529, Japan
Telephone & FAX number: +81-54-238-5134
E-mail address: amhara@ipc.shizuoka.ac.jp

Abstract

Dehydrins are known as plant stress-responsive genes. *Arabidopsis thaliana* has 10 dehydrin genes. Among them, one of the highly expressed genes is a KS-type dehydrin (*At1g54410*). However, the gene product, which is a histidine-rich dehydrin whose molecular mass is 11 kDa (AtHIRD11), has not been studied. Thus, we report the biochemical characterization of the AtHIRD11 protein. Although the AtHIRD11 protein was detected in all organs of *Arabidopsis*, the bolting stem and the flower showed higher accumulation than the other organs, with the AtHIRD11 protein detected in the cambial zone of the stem vasculature. Most of the AtHIRD11 protein was found to be a bound form. The bound AtHIRD11 was solubilized by 1 M NaCl solution. The extracted AtHIRD11 was retained in immobilized metal-affinity chromatography, and eluted by an imidazole gradient. The native AtHIRD11 prepared from *Arabidopsis* was partially phosphorylated, but further phosphorylated by casein kinase 2 *in vitro*. Metal-binding assays indicated that Zn^{2+} may be the best metal for AtHIRD11 binding. These results suggest that AtHIRD11 is a metal-binding dehydrin that shows a house-keeping expression in *Arabidopsis*.

Keywords *Arabidopsis thaliana* - dehydrin - late embryogenesis abundant proteins - metal binding

Abbreviations

ABA abscisic acid

AtHIRD11 *Arabidopsis thaliana* histidine-rich dehydrin whose molecular mass is 11 kDa

CK2 casein kinase 2

2D-PAGE two-dimensional polyacrylamide gel electrophoresis

EDTA ethylenediaminetetraacetic acid

EST expressed sequence tag

IMAC immobilized metal affinity chromatography

PCR polymerase chain reaction

RT-PCR reverse transcription-polymerase chain reaction

SAP shrimp alkaline phosphatase

SDS sodium dodecyl sulfate

SDS-PAGE SDS-polyacrylamide gel electrophoresis

Electronic supplementary material

The online version of this article (doi:xxxxxxxxxxxx) contains supplementary materials, which are available to authorized users.

Introduction

Abiotic stresses such as cold, drought, and high salinity are crucial factors determining plant growth and development. Physiological and molecular alterations systematically occur to respond to these stresses. Such responses have been the subject of many reviews (e.g., Skirycz and Inzé 2010; Hirayama and Shinozaki 2010). Although a large number of genes respond to the abiotic stresses in plants, dehydrins (group 2 late embryogenesis abundant proteins) have been well studied because various plant species possess these genes and produce the respective proteins during embryogenesis and stress responses (Close 1996; Svensson et al. 2002; Rorat 2006; Tunnacliffe and Wise 2007; Battaglia et al. 2008; Hundertmark and Hincha 2008; Hara 2010). Dehydrins possess unique domains called K-, Y-, and S-segments (see reviews cited above). The K-segments (EKKGIMDKIKEKLPG or similar sequences), which are proposed to form an amphipathic helix, are totally conserved in all dehydrins studied so far. The Y-segment (a typical sequence; DEYGNP) and the S-segment (LHRSGSSSSSSSEDD or related sequences) frequently appear in dehydrin sequences. The YSK shorthand is commonly used to classify dehydrins. Because dehydrins are composed of charged and polar amino acids, they are highly hydrophilic and boiling stable (see reviews cited above). Dehydrins are intrinsically unstructured proteins (see reviews cited above). Dehydrins are distributed in a number of subcellular compartments, including the cytoplasm, nucleus, plasma membrane, tonoplast, plastid, mitochondrion, endoplasmic reticulum, and plasmodesmata (see reviews cited above). At the tissue level, dehydrins have been detected mainly in and/or near the vasculature (Godoy et al. 1994; Danyluk et al. 1998; Bravo et al. 1999; Nylander et al. 2001).

Evidence that dehydrins are related to stress tolerance in plants has been reported. Transgenic studies using dehydrin(s) overexpressors have shown that many kinds of dehydrins enhanced tolerance to cold (Hara et al. 2003; Puhakainen et al. 2004; Houde et al. 2004; Yin et al. 2006) and osmotic (Cheng et al. 2002; Figueras et al. 2004; Brini et al. 2007) stresses in various plants. Molecular genetic studies also demonstrated that dehydrin genes were related to cold tolerance

in cowpeas (Ismail et al. 1999). On the one hand, the molecular functions of dehydrins have been discussed. Dehydrins showed cryoprotection (see reviews cited above), antifreeze activity (Wisniewski et al. 1999), phospholipid binding (Koag et al. 2009), and nucleic acid binding (Hara et al. 2009). These activities have been understood to stabilize cellular components in cold and drought conditions. Meanwhile, dehydrins are known to bind metal ions. In the native dehydrin proteins, the S-segments have been shown to be phosphorylated (Plana et al. 1991; Alsheikh et al. 2003; Jiang and Wang 2004; Alsheikh et al. 2005). This phosphorylation promoted calcium binding in the case of the acidic dehydrins (Alsheikh et al. 2005). Dehydrins have also been shown to have an affinity to heavy metals (Svensson et al. 2000; Krüger et al. 2002; Hara et al. 2005) via the histidine-rich domains (Hara et al. 2005).

Arabidopsis thaliana is one of the plants whose dehydrins have been well documented. *Arabidopsis* has 10 dehydrin genes in its genome (Hundertmark and Hincha 2008). Information about the *Arabidopsis* dehydrin genes is summarized in the supplementary material (Fig. S1). Four of the 10 genes, i.e., *COR47* (*At1g20440*, SK_3-type), *ERD10* (*At1g20450*, SK_2-type), *ERD14* (*At1g76180*, SK_2-type), and *RAB18* (*At5g66400*, Y_2SK_2-type), have been well characterized. ERD10, ERD14, and RAB18 proteins were located in the vascular tissues under the control condition, but the expression was expanded to mesophyll tissues when plants were exposed to cold (Nylander et al. 2001). Acidic dehydrins, such as COR47, ERD10, and ERD14, which were detected as phosphorylated forms in plants, could bind to calcium (Alsheikh et al. 2003; Alsheikh et al. 2005). ERD10 and ERD14 showed acidic phospholipid binding (Kovacs et al. 2008), chaperone activity (Kovacs et al. 2008), and cytoskeleton interaction (Abu-Abied et al. 2006). ERD10 was reported to bind water and charged ions (Tompa et al. 2006), and exhibit cryoprotection (Reyes et al. 2008). Besides these analyses, differences of expression degrees between the 10 dehydrin genes in *Arabidopsis* have not been well investigated. When we compared the latest numbers of expressed sequence tags (ESTs) of the *Arabidopsis* dehydrin genes from the TAIR site (http://www.arabidopsis.org/), we found that 5 dehydrins, i.e., *COR47*, *ERD10*, *ERD14*, *RAB18*, and a KS-type dehydrin (*At1g54410*), apparently had a large number

of ESTs (see the supplementary material Fig. S1). Intriguingly, the EST number of the KS-type dehydrin was the largest among the 5 dehydrins. This tendency was confirmed also in the ATTED-II website (http://www.atted.bio.titech.ac.jp). These data suggest that the KS-type dehydrin may be the most expressed dehydrin in the *Arabidopsis* plant. However, no information about the KS-type dehydrin protein has been reported. In this paper, we detected, partially purified, and characterized the *Arabidopsis* KS-type dehydrin protein. Because the KS-type dehydrin is rich in histidine residues (13.3% of total amino acids), we here designate it the *Arabidopsis thaliana* histidine-rich dehydrin whose molecular mass is 11 kDa (AtHIRD11).

Materials and methods

Plant materials

Arabidopsis thaliana (L.) Heynh ecotype Columbia (Col-0) was used. To obtain various organs of *Arabidopsis*, the plants were grown in 6-cm plastic pots containing Peatban (Sakata Seed, Yokohama, Japan) in a 16-h day (120 μmol m^{-2} s^{-1}, fluorescent lamps, FL40SEX-N-HG, NEC, Tokyo, Japan)/8-h night cycle at 22°C in a growth chamber (LH-350S, NK System, Tokyo, Japan). Aerial parts of the plants grown in the same condition were used for cell fractionation, AtHIRD11 purification, and *AtHIRD11* cloning. *Arabidopsis* plants grown under sterile conditions were used to investigate the responses to various chemicals and stresses. The plants were grown on sterile half-strength MS media containing 1% sucrose solidified with 0.8% agar in 90-mm plastic Petri dishes for 12 days in a 16-h day (120 μmol m^{-2} s^{-1})/8-h night cycle at 22°C in a growth chamber. Then, the illumination condition was changed to continuous light (120 μmol m^{-2} s^{-1}) for 4 days in order to acclimatize the plants to the illumination condition of the subsequent stress treatments. For the chemical treatments, 10 plants were transferred to new MS medium containing 100 mM NaCl, 300 mM mannitol, and 10 μM ABA. In order for cold

treatment to be performed, 10 plants were transferred once to the new MS medium in Petri dishes, and the Petri dishes were then placed in a refrigerator (4°C). A drought condition was induced by placing the 10 plants on filter paper at 70% humidity. In this condition, 50% of the initial water content of the plants was lost during the approximately 3-h treatment (data not shown). All treatments were done with 3 sets of plants (1 set consisted of 10 plants). The light condition during the stress treatments was continuous illumination (120 μmol m^{-2} s^{-1} for chemicals and drought, 50 μmol m^{-2} s^{-1} for cold). Whole plants were harvested at 6 and 48 hrs after the treatment, immediately weighed, and kept at -70°C until use.

Protein determination

Soluble protein extracted from plant materials was determined by the Quick Start Bradford Protein Assay (Bio-Rad, Tokyo, Japan). The standard protein was bovine gamma-globulin. Assays were performed according to the manufacturer's instructions. The amounts of protein in the cell debris and organelles were quantified using SDS-PAGE. Suspensions of the cell debris and organelles were resolved by SDS-PAGE, and then the gel was stained with colloidal Coomassie blue (Bio-Safe, Bio-Rad). After the photograph was taken, the total intensity of the proteins contained in the sample was calculated by NIH-Image software. The protein amount was determined from the value of the intensity. The standard protein, bovine gamma-globulin, was used to make a calibration curve.

Immunoblot and immunohistochemical analysis

A polyclonal anti-AtHIRD11 antibody was prepared using a synthetic peptide of E(22)HKKEEEHKKHVDEHKSGE(40) (Fig. 1a, shown by an underline). A conjugate consisting of the peptide and keyhole limpet hemocyanin was injected into rabbits. The antiserum was subjected to an affinity column where the peptide was immobilized. The

affinity-purified antibody was used in this study. Whole plants, organs, and organelles were frozen with liquid N_2 and homogenized with 5 volumes of deionized water at 4°C. The homogenates were directly resolved by 17% SDS-PAGE. After electrophoresis, proteins were blotted onto a polyvinylidene difluoride membrane filter (Immobilon-P, Millipore, Tokyo, Japan) by a Mini Trans-Blot Cell (Bio-Rad). The filter was blocked and incubated with the antibodies by a SNAP i.d. system (Millipore). The primary and secondary antibodies were the anti-AtHIRD11 antibody and horseradish peroxidase conjugated anti-rabbit IgG (GE Healthcare, Tokyo, Japan), respectively. Positive signals were detected using the chemiluminescent Western blotting detection reagent ECL Plus (GE Healthcare). The chemiluminescence was detected by the LAS-4000 imaging system (Fujifilm, Tokyo, Japan).

The *Arabidopsis* bolting stem was used for immunohistochemical analysis of AtHIRD11. The stems were fixed with glutaraldehyde, and then sections were made by a microtome. After dehydration and rehydration with ethanol, the sections were blocked and incubated with antibodies. The primary and secondary antibodies were the anti-AtHIRD11 antibody and alkaline phosphatase-conjugated anti-rabbit IgG (Millipore), respectively. Staining was done with 4-nitro blue tetrazolium chloride and 5-bromo-4-chloro-3-indolyl phosphate. Preimmune serum was used for the control.

Semi-quantification of AtHIRD11 transcripts

The transcript levels of *AtHIRD11* in *Arabidopsis* were analyzed by a semi-quantitative RT-PCR system. Total RNA was extracted from the whole plants with the RNeasy Plant Mini Kit (Qiagen, Tokyo, Japan). One microgram of RNA was subjected to the semi-quantitative RT-PCR system (QuantumRNA 18S Internal Standards Kit, Ambion, TX, USA). In this system, both the target RNA and 18 S rRNA (an internal standard) were amplified together. Reverse transcription was performed at 45°C for 30 min. PCR proceeded through 26 cycles of 94°C for 30 s, 55°C for 30 s, and 72°C for 60 s. The amplified products were analyzed by 3% agarose gel

electrophoresis. After determining the band intensity using NIH-Image software, the relative mRNA contents were deduced from the intensities of the target PCR products and rRNA PCR products according to the instruction manual for the QuantumRNA 18S Internal Standards Kit. The primers were 5'-GATATGGCAGGACTCATCAAC-3' (a sense primer) and 5'-TAAACCAAGATCCAAACC-3' (an antisense primer), which are located in the 5' and 3' non-coding regions of *AtHIRD11*, respectively. The putative sizes of the RT-PCR products for *AtHIRD11* and *18 S rRNA* were 374 bp and 315 bp, respectively.

Cell fractionation by centrifugation

Aerial parts (1 g fresh weight) of 8-week-old *Arabidopsis* plants were homogenized in 5 ml of grinding buffer containing 20 mM MOPS-KOH buffer (pH 7.4), 450 mM sucrose, 1 mM EDTA, 2 mM dithiothreitol, and 1% (w/w) polyvinylpolypyrrolidone by mortar and pestle at 4 °C. The homogenate was filtered through double cheesecloth, and then subjected to differential centrifugations successively at 200x*g* for 1 min, 3,000x*g* for 5 min, 10,000x*g* for 15 min, and 100,000x*g* for 15 min at 4 °C. Pellets formed by the centrifugations were suspended in 5 ml of the grinding buffer. After determination of the protein amount, all fractions were analyzed by immunoblot to detect AtHIRD11 using the anti-AtHIRD11 antibody. The fractions were also tested by immunoblots using marker antibodies, i.e., anti-cytochrome c oxidase subunit II antibody for mitochondria (AgriSera, Vännäs, Sweden) and the anti-D1 reaction centre protein of the photosystem II antibody for chloroplasts (AgriSera).

Extraction condition of AtHIRD11

Aerial parts (200 mg fresh weight) of 4-week-old *Arabidopsis* plants were powdered with liquid N_2 and homogenized in 5 volumes of deionized water. The homogenate was centrifuged at 12,000x*g* for 15 min at 4 °C. To determine the extraction conditions, the pellet in which most

AtHIRD11 existed was resuspended with water solutions containing Triton X-100 (0.1, 0.5, 1, and 2%, w/w), CHAPS (0.1, 0.5, 1, and 2%, w/w), SDS (0.1, 0.5, 1, and 2%, w/w), NaCl (0.25 and 1 M), EDTA (1 and 10 mM), Na_2CO_3 (100 mM), dithiothreitol (10 mM), and metals ($CaCl_2$, $CuCl_2$, $ZnCl_2$, and $FeCl_3$, 10 and 50 mM). Beside that, the pellet was resuspended with water, and then the suspension was treated with heating (65, 80, and 95 °C), freeze and thaw (3 times), and sonication with Sonifier 150 (Branson, CT, USA) in continuous mode 5 for 1 min. The suspensions were incubated for 10 min at room temperature, and then centrifuged as above. The pellet was resuspended with water and the volume was set to the same volume as the supernatant. Both the pellet and the supernatant were analyzed by the immunoblot using the anti-AtHIRD11 antibody.

Purification of AtHIRD11

Aerial parts (5 g fresh weight) of the 8-week-old *Arabidopsis* plants were powdered with liquid N_2 and homogenized in 25 ml deionized water. After centrifuging at 12,000x*g* for 15 min at 4 °C, the pellet was resuspended with the same amount of water, and then centrifuged again. The pellet was resuspended with 1 M NaCl (25 ml). The suspension, which was incubated for 1 h on ice with occasional agitation, was centrifuged as above. The supernatant was applied to a 1-mL HiTrap Chelating HP column (GE Healthcare) immobilizing Cu^{2+}. After washing the column with a running buffer (1/2EQ buffer, 25 mM Tris-HCl buffer pH 7.5 containing 500 mM NaCl), a stepwise gradient of imidazole (20, 100, 250, and 1,000 mM, 4 mL each) based on the 1/2EQ buffer was performed. Fractions containing AtHIRD11 (100 mM imidazole fractions) were combined, and then further purified by gel filtration (NAP-25 column, GE Healthcare). Approximately 50 μg of AtHIRD11 was obtained from 5 g of the plant materials. The protein was identified as AtHIRD11 by nano-liquid chromatography-mass spectrometry/mass spectrometry (nano-LC-MS/MS).

Recombinant AtHIRD11 production

A recombinant protein which has His- and S-tag sequences attached to the N-terminus of AtHIRD11 was produced using the pET-30 *Escherichia coli* expression system (Novagen, WI, USA). First, we prepared the *AtHIRD11* cDNA clone by RT-PCR with the total RNA of *Arabidopsis* using a Takara RNA PCR kit (Takara Bio, Shiga, Japan). The primers of the PCR were 5'-GATATGGCAGGACTCATCAAC-3' (a sense primer) and 5'-TAAACCAAGATCCAAACC-3' (an antisense primer) described as above. The sequence of the clone was identified as the confirmed sequence of At1g54410 published on the TAIR site. The ORF of *AtHIRD11* was inserted into the ligation-independent cloning (LIC) site in accordance with the manufacturer's instructions (Novagen). The primers used for the LIC cloning system were 5'-ggtattgagggtcgcATGgcaggactcatcaac-3' (the sense primer, underlined; the LIC site, capital letters; the start codon of *AtHIRD11*) and 5'-agaggagagttagagccTTAatcgctgtcgctgtc-3' (an antisense primer, underlined; the LIC site, capital letters; the antisense stop codon of *AtHIRD11*). The first methionine of *AtHIRD11* starts directly after the tag, and the translation stops by using the stop codon of *AtHIRD11*. Sequencing the corresponding site of the plasmid indicated that the LIC cloning proceeded correctly. The *E. coli* strain BL21 containing the expression construct was precultured at 37°C. After adding 1 mM isopropyl β-D-thiogalactopyranoside to the culture, the incubation proceeded for an additional 3 h at 28°C. Bacterial cells (800 mL culture) were lysed by treating with BugBuster reagent (Novagen). The lysate was centrifuged at 9,000x*g* for 20 min at 4°C. The supernatant was heated at 90°C for 20 min, and then centrifuged again. The supernatant containing the tagged AtHIRD11 was desalted by the NAP-25 column equilibrated with water. The sample, which was treated with Factor Xa (Novagen) to remove the tags (His- and S-tags), was applied to a 1-mL HiTrap Chelating HP column (GE Healthcare) immobilizing Ni^{2+}. The column was washed with 1/2EQ buffer. AtHIRD11-rich fractions, which were obtained by eluting with a stepwise gradient of imidazole (50, 100, and 150 mM, 9 mL each) based on the

1/2EQ buffer, were desalted, and then further purified using anion-exchange chromatography (DEAE-Toyopearl 650M, Tosoh, Tokyo, Japan) by a linear gradient of NaCl (0-500 mM in 10 mM Tris-HCl buffer pH 7.5). The sample was desalted using the NAP-25 column and freeze-dried. The dried sample was weighed and the AtHIRD11 identified using matrix-assisted laser desorption/ionization-time of flight-mass spectrometry (MALDI-TOF-MS).

MS analysis

The native and recombinant AtHIRD11 proteins were identified by different MS analyses. For the native AtHIRD11, the corresponding band (approximately 16 kDa in size) in the SDS-PAGE gel stained with colloidal Coomassie blue (Bio-Safe, Bio-Rad) was excised to be digested with trypsin. The peptide fragments formed were analyzed by a nano-LC-MS/MS system composed of QSTAR XL (Applied Biosystems, Tokyo, Japan) and Bio NanoLC (KYA Technologies, Tokyo, Japan). The sequences of fragments were matched to the corresponding partial sequences of AtHIRD11 by considering their molecular weights. The matched sequences were IGDALHIGGGNKEGEHK and EGIVDKIK (25% sequence coverage). Traces of other proteins were not detected. For the recombinant AtHIRD11, the purified protein was directly analyzed by using MALDI-TOF-MS. A Voyager DE-STR (Applied Biosystems, Framingham, MA) was operated in the linear mode. A main mass peak was detected and compared to the theoretical molecular weight of AtHIRD11. The calculated mass and experimental mass were 10795.6 and 10795.8, respectively. An additional peak (m/z 11001.1), which may show the matrix (sinapinic acid)-bound AtHIRD11, was also detected.

Phosphorylation analyses

CK2 (New England Biolabs, Tokyo, Japan) and SAP (Takara Bio) were used for phosphorylation and dephosphorylation, respectively. The native protein (0.2 μg) and the

recombinant protein (1 μg) were substrates. CK2 (100 U) and SAP (4 U) were used with corresponding reaction buffers supplied by the manufacturers. The reaction mixtures were incubated for 2 h at 30 °C (CK2) and 2 h at 23 °C (SAP), respectively. The samples were resolved by SDS-PAGE and in some cases by 2D-PAGE. The phosphoproteins were detected using the Pro-Q Diamond Phosphoprotein Gel Staining Kit (Molecular Probes, OR, USA) according to the manufacturer's instructions.

Metal binding assays

Metal binding of AtHIRD11 was judged by means of IMAC using HiTrap Chelating HP columns (1 mL) that chelate Mg^{2+}, Ca^{2+}, Mn^{2+}, Co^{2+}, Ni^{2+}, Cu^{2+}, Zn^{2+}, and Cd^{2+}, respectively. After equilibrating the column with 1/2EQ buffer, the tag-less recombinant AtHIRD11 (2 μM, 100 μL) was applied to the column. The unbound protein was washed out, and then the protein retained in the column was eluted by a linear gradient of imidazole (0-150 mM in 20 mL, the EGP system, Bio-Rad). Fractions (1 mL each) were analyzed by SDS-PAGE. The gel was stained with colloidal Coomassie blue. A HiTrap Chelating HP column charged with no metal was used as a control. The band intensities of AtHIRD11 in the SDS-PAGE gels were calculated using NIH-image software to determine which fraction contained the highest amount of AtHIRD11. The imidazole concentration of the peak fraction was determined from data about the relationship between fraction numbers and imidazole concentrations.

The binding between AtHIRD11 and metals (Co^{2+}, Ni^{2+}, Cu^{2+}, and Zn^{2+}) was analyzed using an ultrafiltration method. Mixtures (final volume; 0.5 mL) containing 16.7 μM AtHIRD11, 10 mM Tris-HCl pH 7.5, 100 mM NaCl, and appropriate concentrations (25-650 μM) of metal chlorides ($CoCl_2$, $NiCl_2$, $CuCl_2$, and $ZnCl_2$) were incubated at 4°C for 10 min. The mixture was subjected to ultrafiltration (Ultrafree-MC, 5000 NMWL, Millipore). The filtration device was centrifuged at 4,000x*g* for 30 min at 4°C. The free metals passed through the filter but the bound ones did not. The concentrations of metals in the filtered solution were determined using a

2-(5-bromo-2-pyridylazo)-5-(N-propyl-N-sulfopropylamino)phenol (5-Br-PAPS) (Dojindo Chemical, Tokyo, Japan) assay. The sample solution (50 µL) was combined with a 20-µM 5-Br-PAPS water solution (450 µL). Absorbance at 540 nm was measured. The linearity was maintained from 0 to 50 µM of each metal. The free metal concentration (F) was used to calculate the bound metal concentration (B). Next, the B/F value and the number of metal atoms bound to AtHIRD11 were determined for each sample. Finally, the Scatchard plots, i.e., the number of metal atoms (x-axis) versus the B/F value (y-axis), were drawn to obtain the values of K_d and B_{max}.

Heat stability and CD

The heat stability of the recombinant AtHIRD11 protein was analyzed. The recombinant AtHIRD11 was dissolved in a phosphate buffer (40 µL) consisting of 13.7 mM NaCl, 0.27 mM KCl, 1 mM Na_2HPO_4, and 0.18 mM KH_2PO_4 (pH 7.4) at the concentration of 0.25 mg mL^{-1}. The solution was heated at 95 °C for 0 (without heating), 5, 10, and 30 min. After cooling to room temperature, the samples were centrifuged at 9,000x*g* for 15 min at room temperature. The pellets were resuspended with the phosphate buffer (40 µL). The supernatants and pellets were subjected to SDS-PAGE. The gel was stained with Coomassie blue. For the control, bovine gamma-globulin was used. The analytical condition of the bovine gamma-globulin was the same as that of AtHIRD11 except that the heat treatment for 30 min was omitted.

The circular dichroism (CD) spectra for AtHIRD11 were collected by using a JASCO (Tokyo, Japan) J-820 spectropolarimeter. The sample was a water solution of AtHIRD11 (0.02 mg mL^{-1}). The scan was performed from 200 to 250 nm. The scan speed and resolution were 20 nm min^{-1} and 0.5 nm, respectively.

Results

Amino acid sequence of AtHIRD11

AtHIRD11 is a small dehydrin consisting of 98 amino acids (Fig. 1a). Although *Arabidopsis* possesses 10 dehydrin genes in its genome, AtHIRD11 is the only KS-type dehydrin (see the supplementary material Fig. S1). AtHIRD11 has a K-segment (HKEGIVDKIKDKIHG, Fig. 1a, shown by the gray background) and an S-segment (SSSSDSDSD, Fig. 1a, shown by the broken underline). A polylysine (PK)-segment (EKKKKKDKKEKK, Fig. 1a, enclosed by an open square) (Hara et al. 2009) is located between the K- and S-segments. Orthologs of AtHIRD11 have been found in various plants, such as ITP of *Ricinus communis*, src1 of *Glycine max*, DHN10 of *Solanum sogarandinum*, wsi724 of *Oryza sativa*, cas15 of *Medicago sativa*, and Grip32 of *Vitis vinifera* (Fig. 1b). Thus, these dehydrins are categorized in the KS-type dehydrin family. The sequence features found in AtHIRD11, e.g. arrangements of the K-, S-, and PK-segments, are conserved in the KS-type dehydrin family. Histidine residues frequently occur over the sequence of AtHIRD11. The histidine content of AtHIRD11 (13.3%) is the 7th highest in the open reading frames of the *Arabidopsis* genome.

Detection of AtHIRD11 protein in Arabidopsis plants

First, we produced a polyclonal anti-AtHIRD11 antibody that was raised against an amino acid sequence of E(22)HKKEEEHKKHVDEHKSGE(40) (Fig. 1a, shown by an underline) to detect AtHIRD11 protein. This sequence is assumed to be specific to the AtHIRD11 protein, because similar sequences were not found in the open reading frames of the *Arabidopsis* genome by a Basic Local Alignment Search Tool (BLAST) search. The specific antibody fraction was purified from the antiserum by affinity chromatography using the EHKKEEEHKKHVDEHKSGE peptide as a ligand. When the total protein extract from the whole *Arabidopsis* plant was subjected to immunoblot analysis, one band whose molecular mass

was about 16 kDa was detected. We later identified the band as the AtHIRD11 protein. Details are given in the section “Extraction and purification of AtHIRD11” below. Thus, it is likely that the antibody specifically recognized the AtHIRD11 protein. The organ distribution of the AtHIRD11 protein was investigated. Although AtHIRD11 protein accumulated in the whole plant, the major sites were the bolting stem and the flower (Fig. 2a, a picture). Relative amounts of the *AtHIRD11* transcripts were estimated using a semi-quantitative reverse transcription-polymerase chain reaction (RT-PCR) system. The *AtHIRD11* transcripts were detected in all organs (Fig. 2a, a graph). The tests of the stress dependency of the AtHIRD11 protein indicated that the AtHIRD11 protein level was not influenced by NaCl (Fig. 2c), cold (Fig. 2d), mannitol (Fig. 2e), or ABA (abscisic acid, Fig. 2g). Drought decreased the protein level (Fig. 2f). The *AtHIRD11* transcript levels did not apparently change under these stress conditions. This shows that AtHIRD11 protein is unlikely to be up-regulated by stresses at the transcriptional and translational levels.

Immunohistochemistry using the anti-AtHIRD11 antibody indicated that AtHIRD11 was detected in the cambial zone of the vasculature (Fig. 3a and c). When plants were exposed to cold, drought, NaCl, and ABA, the sites and degrees of the immunostaining did not change (data not shown). The following tests were done to determine the subcellular localization of AtHIRD11. At first, aerial parts of the *Arabidopsis* plant were homogenized with an organelle-isolation buffer containing sucrose (450 mM) as an osmolyte. After the homogenate was centrifuged at 12,000 g for 10 min, most AtHIRD11 was found in the pellet and little was in the supernatant (Fig. 4, lanes P and S). This result was obtained when the buffer was changed to low osmotic buffers and even water (data not shown). This indicates that most AtHIRD11 may exist in the centrifugation pellet, which contains cell debris and organelles such as plastids, mitochondria, and peroxisomes, and that AtHIRD11 may tightly bind to the pellet. The centrifugation fractionation showed that AtHIRD11 was mostly detected in the 3,000P fraction (Fig. 4, lane B), whereas a very small amount of AtHIRD11 was also found in the 100,000P fraction (Fig. 4, lane D). In the series of centrifugations (Fig. 4, lanes A-E), the cytochrome c

oxidase subunit II (COX II, a mitochondrial marker) and the D1 reaction center protein of photosystem II (PsbA, a plastidial marker) were mainly found in the 3,000P fraction (Fig. 4, lane B), suggesting that the 3,000P fraction contains mitochondria and plastids. We further examined which organelle(s) AtHIRD11 bound to, using discontinuous density gradient centrifugation techniques. However, we have not been able to determine the AtHIRD11-bound organelles. Transient expression of the *AtHIRD11-green fluorescent protein* (*GFP*) and *GFP-AtHIRD11* chimera genes in onion (*Allium cepa*) epidermal cells suggested that the corresponding chimera proteins were located in the cytoplasm and nucleus (see the supplementary material Fig. S2). The fluorescence patterns of the chimera proteins were similar to that of the non-chimeric GFP alone.

Extraction and purification of AtHIRD11

To characterize the AtHIRD11 protein, we attempted to extract AtHIRD11 from *Arabidopsis* plants. The vast majority of AtHIRD11 was found in the pellet formed when the plant homogenate was centrifuged at 12,000x*g* (Fig. 4, lane P). Thus, we used the pellet to extract AtHIRD11. Since some dehydrins were extracted from membrane fractions by the nonionic detergent Triton X-100 (0.2%) (Alsheikh et al. 2003; Alsheikh et al. 2005; Heyen et al. 2002), we first selected this extraction method. Although Triton X-100 was added to the sediment at the concentrations of 0.1-2%, AtHIRD11 could not be extracted (Fig. 5a, Triton X). The zwitterionic detergent 3-[3-(cholamidopropyl)dimethylammonio]-1-propane sulfonate (CHAPS, up to 2%) was also not effective for AtHIRD11 extraction (data not shown). The anionic detergent sodium dodecyl sulfate (SDS), however, could solubilize AtHIRD11 at the concentration of 2% (Fig. 5a, SDS). Various reagents, such as NaCl (up to 1 M), ethylenediaminetetraacetic acid (EDTA, up to 10 mM), and Na_2CO_3 (100 mM) were tested to extract AtHIRD11 (Fig. 5, NaCl, EDTA, and Na_2CO_3). Among these compounds, only NaCl (1 M) efficiently solubilized AtHIRD11. Dithiothreitol (10 mM), metals ($CaCl_2$, $CuCl_2$, $ZnCl_2$, and

$FeCl_3$, up to 50 mM), and physical treatments (heating, freeze and thaw, and sonication) were not effective; AtHIRD11 was extracted only by SDS and NaCl. Considering the convenience of the subsequent purification step, we decided to use NaCl for the AtHIRD11 extraction.

Immobilized metal affinity chromatography (IMAC) was used for the first step of purification, because the histidine content of AtHIRD11 is high as described above. When proteins extracted from the 12,000 g pellet with NaCl solution were applied to the Cu^{2+}-chelating column, AtHIRD11 was retained in the column. After washing the column with a running buffer, an apparent protein band whose molecular mass was about 16 kDa was eluted with the stepwise gradient of imidazole (Fig. 5b, lane 3). Immunoblot analyses showed that the protein was recognized by the anti-AtHIRD11 antibody (Fig. 5c, lane 3), indicating that the protein is likely to be AtHIRD11. The fractions containing AtHIRD11 were combined, and then further purified by gel filtration. The nano-LC-MS/MS analysis of the protein band showed that the AtHIRD11-related sequences, i.e., I(8)GDALHIGGGNKEGEHK(24) and E(43)GIVDKIK(50), were identified. These results demonstrate that the band is the AtHIRD11 protein.

Phosphorylation of AtHIRD11

Since some dehydrins were phosphorylated (Plana et al. 1991; Alsheikh et al. 2003; Alsheikh et al. 2005; Heyen et al. 2002; Röhrig et al. 2006), we investigated whether AtHIRD11 purified from *Arabidopsis* was phosphorylated. Staining the gel with a Pro-Q diamond dye, which detects phosphorylated proteins, revealed that the native AtHIRD11 purified from *Arabidopsis* may be phosphorylated (Fig. 6). The signal intensity of the native AtHIRD11 stained with the Pro-Q diamond was enhanced by casein kinase 2 (CK2), but was reduced by shrimp alkaline phosphatase (SAP), suggesting that the phosphorylation state of the native AtHIRD11 was partial. A recombinant AtHIRD11 protein that was not phosphorylated was apparently phosphorylated by CK2. The phosphorylation of the recombinant AtHIRD11 by CK2 was cancelled by the SAP treatment (data not shown). The electrophoretic mobility of the

recombinant AtHIRD11 protein phosphorylated by CK2 was slightly smaller than that of the unphosphorylated recombinant AtHIRD11. The native AtHIRD11 was also analyzed using two-dimensional polyacrylamide gel electrophoresis (2D-PAGE). Detection of AtHIRD11 by colloidal Coomassie blue staining, immunoblot, and Pro-Q diamond staining indicated that the native AtHIRD11 assumed multiple forms, some of which were phosphorylated (Fig. 7, NP). When the native AtHIRD11 was treated with SAP, the multiple forms turned into approximately two major forms whose isoelectric points were near 7.0 (Fig. 7, NS). Since the calculated isoelectric point of AtHIRD11 is 6.8, the SAP-treated proteins are likely to be dephosphorylated. Similar forms were observed in the recombinant AtHIRD11 (Fig. 7, RP). It is unknown why more forms than one were found in the SAP-treated AtHIRD11 and the recombinant AtHIRD11.

Metal binding of AtHIRD11

As mentioned above, the native AtHIRD11 was retained on the Cu^{2+}-chelating column. However, the native AtHIRD11 was not retained on the Ca^{2+}-chelating column (data not shown). This suggests that AtHIRD11 may show a specific metal binding. Because the native AtHIRD11 consists of multiple forms at least partially due to phosphorylation, it is difficult to individually analyze metal-binding properties in each form. Thus, we used the recombinant AtHIRD11, which was not phosphorylated by CK2. At first, IMAC was performed to investigate whether AtHIRD11 can bind metals, such as Mg^{2+}, Ca^{2+}, Mn^{2+}, Co^{2+}, Ni^{2+}, Cu^{2+}, Zn^{2+}, and Cd^{2+} (Fig. 8a). Such IMAC assays have been used to evaluate the strength of the metal binding of proteins via histidine residues (Ueda et al. 2003). AtHIRD11 was shown to be retained on the columns immobilizing Co^{2+}, Ni^{2+}, Cu^{2+}, and Zn^{2+}. However, AtHIRD11 passed through the columns immobilizing Mg^{2+}, Ca^{2+}, Mn^{2+}, and Cd^{2+}. AtHIRD11 was eluted from the Co^{2+}-chelating column with imidazole at the concentration of approximately 25 mM. The elution of AtHIRD11 from the Ni^{2+}-, Cu^{2+}-, and Zn^{2+}-chelating columns occurred when the imidazole concentration reached 32-37 mM.

Binding modes between the recombinant AtHIRD11 and Co^{2+}, Ni^{2+}, Cu^{2+}, or Zn^{2+} were analyzed by the equilibrium methods. The bindings of AtHIRD11 to these four metals showed two-phase binding patterns, whereas dissociation constants (K_d) and maximum binding capacities (B_{max}) were different among the metal species (Fig. 8b). The K_ds of higher-affinity bindings were 4.8 μM (Co^{2+}), 2.8 μM (Ni^{2+}), 3.3 μM (Cu^{2+}), and 1.4 μM (Zn^{2+}), respectively. The B_{max}s were 2.2 mol Co^{2+}, 4.9 mol Ni^{2+}, 7.8 mol Cu^{2+}, and 7.9 mol Zn^{2+} per mol AtHIRD11, respectively. These data show that AtHIRD11 may prefer Zn^{2+} most, while the values of K_ds and B_{max}s were not very different among the four metals tested.

Disorder of the AtHIRD11 protein

It has been reported that dehydrins are disordered proteins (see reviews cited in the Introduction section). In order to show whether AtHIRD11 is a disordered protein, we applied techniques for recognizing protein disorder (Tompa 2009). In this study, we performed the heat stability test, circular dichroism (CD) analysis, and computer prediction (IUPred, http://iupred.enzim.hu/). First, the heat stability of the recombinant AtHIRD11 protein was investigated (Fig. 9a). AtHIRD11 was kept soluble during heat treatment for 30 min. Inversely, bovine gamma-globulin, which is a typical globular protein, was aggregated by the heat treatment and precipitated by centrifugation. Second, the CD analysis indicated that the recombinant AtHIRD11 was disordered because the large negative peak at 205 nm occurred (Fig. 9b). Third, AtHIRD11 showed a high disorder tendency through the sequence when its amino acid sequence was inputted to the IUPred web server (see the supplementary material Fig. S3). These data suggest that AtHIRD11 is a disordered protein. In addition, AtHIRD11 showed an unusual mobility in SDS-polyacrylamide gel electrophoresis (SDS-PAGE). Although the calculated molecular weight of AtHIRD11 is 10.8 kDa, the experimental size of AtHIRD11, which is predicted by its mobility in the SDS-PAGE analyses (e.g. Fig. 5b), was approximately 16 kDa. Such differences have been observed in many intrinsically disordered proteins (Tompa 2009).

Taken together, these findings show that it is likely that AtHIRD11 is a disordered protein.

Discussion

The *AtHIRD11* (*At1g54410*) gene encodes a KS-type dehydrin that is widely distributed in higher plants. Many orthologs have been found in various plant species, such as *Medicago sativa* (*cas15*, accession number: L12462), *Oryza sativa* (*wsi724*, accession number: D26538), *Glycine max* (*src1*, accession number: AB000129), *Vitis vinifera* (*Grip32*, accession number: CAB85631), *Ricinus communis* (*ITP*, accession number: CAC84735) (Krüger et al. 2002), and *Solanum sogarandinum* (*DHN10*, accession number: AAN37899) (Rorat et al. 2004). It is noteworthy that *AtHIRD11* is one of the most constitutively expressed dehydrin genes in *Arabidopsis*, because the TAIR site represents that *AtHIRD11* has the highest EST number among the *Arabidopsis* dehydrins. In addition, the eFP *Arabidopsis* browser (http://bbc.botany.utoronto.ca), the ATTED-II website, and a recent paper (Hundertmark and Hincha 2008) showed that alteration of the *AtHIRD11* gene expression by stresses was not significant. These results suggest that the *AtHIRD11* gene is constitutively expressed in *Arabidopsis*. In this study, we detected the AtHIRD11 protein using a specific antibody. Although drought reduced the AtHIRD11 level, no stimuli could remarkably enhance the AtHIRD11 accumulation. This indicates that in most cases the AtHIRD11 protein is constitutively expressed in *Arabidopsis*. The eFP site states that the *AtHIRD11* gene is expressed in the whole plant. However, we found that the AtHIRD11 protein mainly accumulated in the bolting stem and flower of *Arabidopsis* despite its detection throughout the plant. This suggests that tissue-specific post-transcriptional regulation may occur in AtHIRD11 production.

It has been believed that most dehydrins are extracted as soluble proteins. Some dehydrins, which are weakly associated with the endomembranes, have shown to be solubilized with a low concentration of the nonionic detergent Triton X-100 (Alsheikh et al. 2003; Alsheikh et al. 2005;

Heyen et al. 2002). Unlike these cases, most AtHIRD11 was found to bind tightly to the pellet of a tissue homogenate obtained by a low-gravity centrifugation (3,000x*g*). Although we hypothesized that the AtHIRD11 protein may be located in some organelle(s), unfortunately, we could not define the organelle(s).

The *Ricinus* ITP protein, which is an ortholog of AtHIRD11, was detected in the phloem exudate of the seedlings (Krüger et al. 2002). Since ITP binds to metals, the protein is proposed to be a metal transporter that moves through the phloem of young plants. On the other hand, immunohistochemical analysis demonstrated that the accumulation of AtHIRD11 was most detected in the cambial zone of the vasculature of the stem (Fig. 3). Moreover, most AtHIRD11 was found to be immobilized, suggesting that AtHIRD11 may not function as a metal transporter at least in the phloem of adult *Arabidopsis*. It is unknown how AtHIRD11 bound to the pellet fraction. Since AtHIRD11 was efficiently extracted by NaCl, an ionic bond may participate in the binding. Membrane-bound acidic dehydrins, such as ERD10, ERD14, COR47, and VCaB45, were efficiently solubilized by a low concentration of Triton X-100 (0.2%) (Alsheikh et al. 2003; Alsheikh et al. 2005; Heyen et al. 2002), suggesting that these dehydrins may be weakly associated to the membrane surface by hydrophobic interactions. It is suggested that dehydrins may interact with subcellular architectures by various binding modes.

It was demonstrated that AtHIRD11 is a metal-binding protein. The recombinant AtHIRD11 bound to Co^{2+}, Ni^{2+}, Cu^{2+}, and Zn^{2+} but not to Mg^{2+}, Ca^{2+}, Mn^{2+}, and Cd^{2+}. This tendency was similar to the metal-binding characteristics of CuCOR15 (a K_2S-type) (Hara et al. 2005). On the other hand, acidic dehydrins (ERD10, ERD14, COR47, and VCaB45) could bind to Ca^{2+}, and the binding was enhanced when they were phosphorylated (Alsheikh et al. 2003; Alsheikh et al. 2005; Heyen et al. 2002). However, a neutral dehydrin RAB18 could not bind to Ca^{2+} even when the dehydrin was phosphorylated (Alsheikh et al. 2005). In the present study, neither the unphosphorylated AtHIRD11 (the recombinant protein) nor the phosphorylated AtHIRD11 (the native protein) bound to Ca^{2+}. This result may be due to that AtHIRD11 is a neutral dehydrin like RAB18. Although it has been discussed that Ca^{2+} binding of acidic dehydrins may be

related to signaling and sequestering Ca^{2+}, AtHIRD11 may not directly contribute to such Ca^{2+}-dependent events.

Generally, dehydrins are distributed in and/or near the vascular tissues (Godoy et al. 1994; Danyluk et al. 1998; Bravo et al. 1999; Nylander et al. 2001). *Arabidopsis* ERD10, ERD14, LTI30, and RAB18 were found in xylem and phloem (Nylander et al. 2001). When *Arabidopsis* plants were exposed to the cold and to exogenous ABA, the staining intensity of these dehydrins increased, and their distribution extended over the non-vascular tissues. Although AtHIRD11 was also found in the vascular tissue, the distribution and the accumulation degree did not alter when various stimuli such as cold, ABA, drought, and NaCl were applied to the plants. These results indicate that AtHIRD11 shows unique patterns of expression different from other *Arabidopsis* dehydrins, suggesting that AtHIRD11 may be a house-keeping dehydrin.

Here, we biochemically characterized the AtHIRD11 protein from *Arabidopsis*. Since some characteristics of the AtHIRD11 protein were different from those of other dehydrins, the KS-type dehydrins may have specific biochemical roles in plants.

Acknowledgment

This work was supported by a Grant-in-Aid for Scientific Research from the Ministry of Education, Science and Culture of Japan (19380182).

References

Abu-Abied M, Golomb L, Belausov E, Huang S, Geiger B, Kam Z, Staiger CJ, Sadot E (2006) Identification of plant cytoskeleton-interacting proteins by screening for actin stress fiber association in mammalian fibroblasts. Plant J 48:367-379.

Alsheikh MK, Heyen BJ, Randall SK (2003) Ion binding properties of the dehydrin ERD14 are dependent upon phosphorylation. J Biol Chem 278:40882-40889

Alsheikh MK, Svensson JT, Randall SK (2005) Phosphorylation regulated ion-binding is a

property shared by the acidic subclass dehydrins. Plant Cell Environ 28:1114-1122

Battaglia M, Olvera-Carrillo Y, Garciarrubio A, Campos F, Covarrubias AA (2008) The enigmatic LEA proteins and other hydrophilins. Plant Physiol 148:6-24

Bravo LA, Close TJ, Corcuera LJ, Guy CL (1999) Characterization of an 80-kDa dehydrin-like protein in barley responsive to cold acclimation. Physiol Plant 106:177-183

Brini F, Hanin M, Lumbreras V, Amara I, Khoudi H, Hassairi A, Pagès M, Masmoudi K (2007) Overexpression of wheat dehydrin DHN-5 enhances tolerance to salt and osmotic stress in *Arabidopsis thaliana*. Plant Cell Rep 26:2017-2026

Cheng Z, Targolli J, Huang X, Wu R (2002) Wheat LEA genes, PMA80 and PMA1959 enhance dehydration tolerance of transgenic rice (*Oryza sativa* L.). Mol Breed 10:71-82

Close TJ (1996) Dehydrins: Emergence of a biochemical role of a family of plant dehydration proteins. Physiol Plant 97:795-803

Danyluk J, Perron A, Houde M, Limin A, Fowler B, Benhamou N, Sarhan F (1998) Accumulation of an acidic dehydrin in the vicinity of the plasma membrane during cold acclimation of wheat. Plant Cell 10:623-638

Figueras M, Pujal J, Saleh A, Save R, Pagès M, Goday A (2004) Maize Rabl7 overexpression in *Arabidopsis* plants promotes osmotic stress tolerance. Ann Appl Biol 144:251-257

Godoy JA, Lunar R, Torres-Schumann S, Moreno J, Rodrigo RM, Pintor-Toro JA (1994) Expression, tissue distribution and subcellular localization of dehydrin TAS14 in salt-stressed tomato plants. Plant Mol Biol 26:1921-1934

Hara M (2010) The multifunctionality of dehydrins: An overview. Plant Signal Behav 5:503-508

Hara M, Fujinaga M, Kuboi T (2005) Metal binding by citrus dehydrin with histidine-rich domains. J Exp Bot 56:2695-2703

Hara M, Shinoda Y, Tanaka Y, Kuboi T (2009) DNA binding of citrus dehydrin promoted by zinc ion. Plant Cell Environ 32:532-541

Hara M, Terashima S, Fukaya T, Kuboi T (2003) Enhancement of cold tolerance and inhibition of lipid peroxidation by citrus dehydrin in transgenic tobacco. Planta 217:290-298

Heyen BJ, Alsheikh MK, Smith EA, Torvik CF, Seals DF, Randall SK (2002) The calcium-binding activity of a vacuole-associated, dehydrin-like protein is regulated by phosphorylation. Plant Physiol 130:675-687

Hirayama T, Shinozaki K (2010) Research on plant abiotic stress responses in the post-genome era: past, present and future. Plant J 61:1041-1052

Houde M, Dallaire S, N'Dong D, Sarhan F (2004) Overexpression of the acidic dehydrin WCOR410 improves freezing tolerance in transgenic strawberry leaves. Plant Biotechnol J 2:381-387

Hundertmark M, Hincha DK (2008) LEA (Late Embryogenesis Abundant) proteins and their encoding genes in *Arabidopsis thaliana*. BMC Genom 9:118

Ismail AM, Hall AE, Close TJ (1999) Allelic variation of a dehydrin gene cosegregates with chilling tolerance during seedling emergence. Proc Natl Acad Sci USA 96:13566-13570

Jiang X, Wang Y (2004) β-Elimination coupled with tandem mass spectrometry for the identification of in vivo and in vitro phosphorylation sites in maize dehydrin DHN1 protein. Biochemistry 43:15567-15576

Koag MC, Wilkens S, Fenton RD, Resnik J, Vo E, Close TJ (2009) The K-segment of maize DHN1 mediates binding to anionic phospholipid vesicles and concomitant structural changes. Plant Physiol 150:1503-1514

Kovacs D, Kalmar E, Torok Z, Tompa P (2008) Chaperone activity of ERD10 and ERD14, two disordered stress-related plant proteins. Plant Physiol 147:381-390

Krüger C, Berkowitz O, Stephan UW, Hell R (2002) A metal-binding member of the late embryogenesis abundant protein family transports iron in the phloem of *Ricinus communis* L. J Biol Chem 277:25062-25069

Nylander M, Svensson J, Palva ET, Welin BV (2001) Stress-induced accumulation and tissue-specific localization of dehydrins in *Arabidopsis thaliana*. Plant Mol Biol 45:263-279

Plana M, Itarte E, Eritja R, Goday A, Pages M, Martinez MC (1991) Phosphorylation of the maize RAB-17 protein by casein kinase 2. J Biol Chem 266:22510-22514

Puhakainen T, Hess MW, Mäkelä P, Svensson J, Heino P, Palva ET (2004) Overexpression of multiple dehydrin genes enhances tolerance to freezing stress in Arabidopsis. Plant Mol Biol 54:743-753

Reyes JL, Campos F, Wei H, Arora R, Yang Y, Karlson DT, Covarrubias AA (2008) Functional dissection of hydrophilins during in vitro freeze protection. Plant Cell Environ 31:1781-1790

Röhrig H, Schmidt J, Colby T, Bräutigam A, Hufnagel P, Böhm N, Bartels D (2006) Desiccation

of the resurrection plant *Craterostigma plantagineum* induces dynamic changes in protein phosphorylation. Plant Cell Environ 29:1606-1615

Rorat T (2006) Plant dehydrins: tissue location, structure and function. Cell Mol Biol Lett 11:536-556

Rorat T, Grygorowicz WJ, Irzykowski W, Rey P (2004) Expression of KS-type dehydrins is primarily regulated by factors related to organ type and leaf developmental stage during vegetative growth. Planta 218:878-885

Skirycz A, Inzé D (2010) More from less: plant growth under limited water. Curr Opin Biotechnol 21:197-203

Svensson J, Ismail AM, Palva ET, Close TJ (2002) Dehydrins. In: Storey KB, Storey JM (eds) Sensing, Signaling and Cell Adaptation, Elsevier, Amsterdam, pp 155-171

Svensson J, Palva ET, Welin B (2000) Purification of recombinant *Arabidopsis thaliana* dehydrins by metal ion affinity chromatography. Protein Expr Purif 20:169-178

Tompa P (2009) Structure and function of intrinsically disordered proteins. CRC Press, Florida

Tompa P, Bánki P, Bokor M, Kamasa P, Kovács D, Lasanda G, Tompa K (2006) Protein-water and protein-buffer interactions in the aqueous solution of an intrinsically unstructured plant dehydrin: NMR intensity and DSC aspects. Biophys J 91:2243-2249

Tunnacliffe A, Wise MJ (2007) The continuing conundrum of the LEA proteins. Naturwissenschaften 94:791-812

Ueda EKM, Gout PW, Morganti L (2003) Current and prospective applications of metal ion-protein binding. J Chromatogr A 988:1-23

Wisniewski M, Webb R, Balsamo R, Close TJ, Yu XM, Griffith M (1999) Purification, immunolocalization, cryoprotective, and antifreeze activity of PCA60: A dehydrin from peach (*Prunus persica*). Physiol Plant 105:600-608

Yin Z, Rorat T, Szabala BM, Ziólkowska A, Malepszy S (2006) Expression of a *Solanum sogarandinum* SK3-type dehydrin enhances cold tolerance in transgenic cucumber seedlings. Plant Sci 170:1164-1172

Figure legends

Fig. 1. Sequence data of AtHIRD11. (**a**) Amino acid sequence of AtHIRD11. Underline, peptide sequence to produce anti-AtHIRD11 antibody; grey background, K-segment; open square, polylysine (PK)-segment; broken underline, S-segment. (**b**) KS-type dehydrins. ITP (accession number: CAC84735), src1 (accession number: AB000129), DHN10 (accession number: AAN37899), wsi724 (accession number: D26538), AtHIRD11 (code number: At1g54410, in this study), cas15 (accession number: L12462), and Grip32 (accession number: CAB85631). Phylogenetic tree was produced by using an unweighted pair group method using arithmetic averages (UPGMA) at the amino acid level.

Fig. 2. Detection of AtHIRD11 in *Arabidopsis*. The AtHIRD11 protein and its transcript were analyzed by using immunoblot (pictures) and semi-quantitative reverse transcription-polymerase chain reaction (RT-PCR, graphs), respectively. (**a**) Organ distribution of AtHIRD11. Whole pre-bolting plants (A), rosettes of bolting plants (B), flowering stems (C), cauline leaves (D), flowers (E), siliques (F), and roots (G). Effects of stresses on AtHIRD11 expression. Control (**b**), NaCl (**c**), cold (**d**), mannitol (**e**), drought (**f**), and ABA (**g**). Plants were harvested 0, 6, and 48 h after the treatments. In the immunoblots (pictures), crude proteins (5 μg) were loaded. Arrowheads indicate the position of the AtHIRD11 protein. To judge the significant differences in signal intensities between the bands in each blot, 3 individual protein samples obtained from 3 different sets of plants were subjected to the immunoblots. After the band intensities were determined, a mean and SE (n=3) of each organ or each treatment were calculated. Student's t test at $P = 0.05$ was applied. * Significant difference at the $P < 0.05$ level. To determine *, the values of lane B (immunoblot **a**) and lane 0 h (immunoblots **b**-**g**) were standardized. In the results for transcript analyses (graphs **a**-**g**), the values and bars represent the means and SDs of 3 measurements, respectively. We did not judge significant differences, because the values in this experiment were produced by the semi-quantitative method.

Fig. 3. Immunohistochemical analyses of AtHIRD11 in the flowering stem of *Arabidopsis*. Transverse sections were examined using the anti-AtHIRD11 antibody (**a** and **c**) and preimmune antiserum (**b** and **d**). Phloem (p), cambial zone (cz), and xylem (x) are shown. White and black bars indicate 0.2 and 0.15 mm, respectively.

Fig. 4. Differential centrifugation fractionation of *Arabidopsis* plants. Aerial parts of the plant were homogenized with an organelle-isolation buffer. The homogenate was used for the following centrifugation fractionations. Pellet (lane P) and supernatant (lane S) were obtained by centrifuging the homogenate at 12,000x*g*. The homogenate was also subjected to stepwise centrifugations. Pellets were prepared by sequential centrifugation at 200x*g* (lane A), 3,000x*g* (3,000P, lane B), 10,000x*g* (lane C), and then 100,000x*g* (100,000P, lane D). The supernatant of the final centrifugation at 100,000x*g* was also used (lane E). Fractions (5 μg protein for lanes P and S; 0.5 μg protein for lanes A-E) were loaded. The primary antibodies were anti-AtHIRD11 antibody, anti-cytochrome c oxidase subunit II (COX II, mitochondria marker) antibody, and the anti-D1 reaction center protein of the photosystem II (PsbA, chloroplasts marker) antibody.

Fig. 5. Extraction and partial purification of AtHIRD11 from *Arabidopsis* plants. Extraction of AtHIRD11 (**a**). Pellets of plant homogenates were resuspended with deionized water, NaCl (1 M), EDTA (10 mM), Na_2CO_3 (100 mM), Triton X-100 (2%, w/w), and SDS (2%, w/w). Then the suspensions were centrifuged. Pellets formed by the centrifugation were resuspended again with an equal volume of deionized water. The resuspended pellets (lanes P) and supernatants (lanes S) were analyzed by immunoblot using anti-AtHIRD11 antibody. Proteins in each purification step were analyzed by SDS-PAGE (**b**) and immunoblot (**c**). The SDS-PAGE gels were stained with Coomassie blue. Anti-AtHIRD11 antibody was used for the immunoblot. Lane 1, pellets of plant homogenates (1 μg protein for **b** and 100 ng protein for **c**); lane 2, NaCl-extracted fraction (1 μg protein for **b** and 100 ng protein for **c**); lane 3, fraction after Cu^{2+}-chelating column (0.5 μg protein for **b** and 50 ng protein for **c**). Arrowheads indicate the

positions of AtHIRD11.

Fig. 6. Phosphorylation and dephosphorylation of AtHIRD11. Native and recombinant AtHIRD11 proteins were phosphorylated by CK2 and dephosphorylated by SAP. Mock and enzymatic treatments are represented by - and +, respectively. NP, native AtHIRD11; RP, recombinant AtHIRD11; white circles, proteins derived from CK2 reagent; white arrowheads, proteins derived from SAP reagent. Amounts of loaded samples are 200 ng protein (native AtHIRD11) and 1 μg protein (recombinant AtHIRD11), respectively. Black arrowheads indicate the positions of AtHIRD11. Gels were stained with Coomassie blue and Pro-Q.

Fig. 7. Separation of AtHIRD11 proteins using 2D-PAGE. Native AtHIRD11 untreated (NP), native AtHIRD11 treated with SAP (NS), and recombinant AtHIRD11 (RP). Results of Coomassie staining, immunoblot, and Pro-Q staining are shown.

Fig. 8. Metal binding of AtHIRD11. Results of IMAC (**a**). Recombinant AtHIRD11 was applied to columns immobilizing Mg^{2+}, Ca^{2+}, Mn^{2+}, Co^{2+}, Ni^{2+}, Cu^{2+}, Zn^{2+}, and Cd^{2+}. After washing the columns, elution by an imidazole gradient was performed. The imidazole concentration in the fraction that contained the largest amount of AtHIRD11 was determined. NM represents the no-metal control. Values and bars represent means and SD of three measurements, respectively. * No significant difference; ** significant difference at the $P < 0.05$ level. To determine * or **, the value of the Ni^{2+} column was standardized. Determination of dissociation constants (K_d) and maximum binding capacities (B_{max}) using Scatchard plots (**b**). K_ds of higher affinity bindings and that of lower affinity bindings are shown. B_{max}s are also indicated. Means and SD were produced by three measurements.

Fig. 9. Heat stability and CD spectrum of AtHIRD11. Heat stabilities of the recombinant AtHIRD11and bovine gamma-globulin were analyzed (**a**). AtHIRD11 and bovine

gamma-globulin were dissolved in a phosphate buffer (0.25 mg mL^{-1}). The solutions were heated at 95 °C for the corresponding periods. After cooling, the samples were centrifuged, and then the pellets were resuspended with an equal volume of the phosphate buffer. The supernatants (S) and resuspended pellets (P) were analyzed by SDS-PAGE. Closed and open arrowheads indicate AtHIRD11 and bovine gamma-globulin, respectively. Circular dichroism (CD) spectrum for the recombinant AtHIRD11 (**b**). Dots show the means of three measurements.

Supplementary Fig. S1. *Arabidopsis* dehydrins. Ten dehydrins have been found in the *Arabidopsis* genome. Gene codes, gene names, arrangements of segments, and EST numbers found in the TAIR site (http://www.arabidopsis.org/) are shown. * This study.

Supplementary Fig. S2. Subcellular localization of AtHIRD11. *Green fluorescent protein* (*GFP*)-related constructs were transiently expressed in onion (*Allium cepa*) epidermal cells. (**a**) The *AtHIRD11-GFP* expression construct (*35S-Ω-AtHIRD11-sGFP*). (**b**) The *GFP-AtHIRD11* expression construct (*35S-Ω-sGFP-AtHIRD11*). (**c**) The *GFP* expression construct (*35S-Ω-sGFP*). White bars represent 100 μm. The constructs were transiently expressed in onion epidermal cells using particle bombardment (PDS-1000, Bio-Rad). Fluorescent cells were imaged by confocal laser-scanning microscopy (TCS SL, Leica, Tokyo, Japan).

Supplementary Fig. S3. Prediction of disorder of AtHIRD11 by using IUPred (http://iupred.enzim.hu/). The result of the prediction is represented. AtHIRD11 shows a high disorder tendency through the sequence. The amino acid sequence of AtHIRD11 is exhibited.

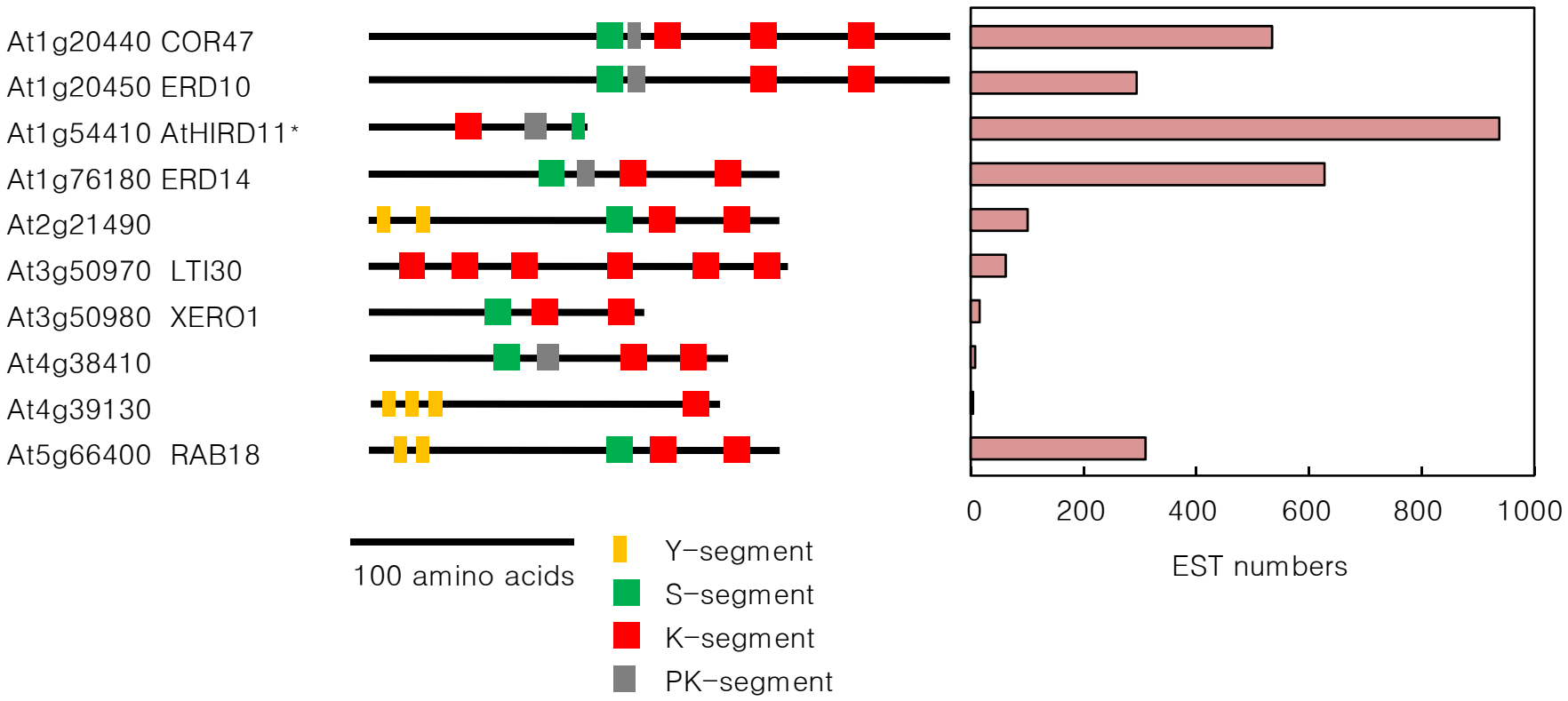

Supplementary Fig. S1. *Arabidopsis* dehydrins. Ten dehydrins have been found in the *Arabidopsis* genome. Gene codes, gene names, arrangements of segments, and EST numbers found in the TAIR site (http://www.arabidopsis.org/) are shown. * This study.

Biochemical characterization of the Arabidopsis KS-type dehydrin protein, whose gene expression is constitutively abundant rather than stress dependent. Hara et al., amhara@ipc.shizuoka.ac.jp

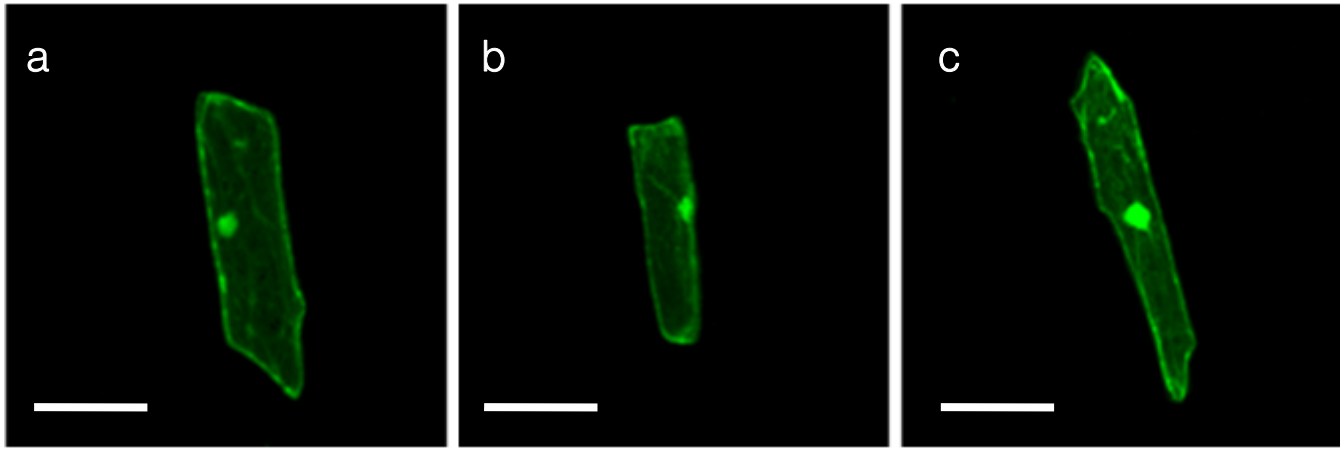

Supplementary Fig. S2. Subcellular localization of AtHIRD11. *Green fluorescent protein* (*GFP*)-related constructs were transiently expressed in onion (*Allium cepa*) epidermal cells. (a) The *AtHIRD11-GFP* expression construct (*35S-Ω-AtHIRD11-sGFP*). (b) The *GFP-AtHIRD11* expression construct (*35S-Ω-sGFP-AtHIRD11*). (c) The *GFP* expression construct (*35S-Ω-sGFP*). White bars represent 100 μm. The constructs were transiently expressed in onion epidermal cells using particle bombardment (PDS-1000, Bio-Rad). Fluorescent cells were imaged by confocal laser-scanning microscopy (TCS SL, Leica, Tokyo, Japan).

Biochemical characterization of the Arabidopsis KS-type dehydrin protein, whose gene expression is constitutively abundant rather than stress dependent. Hara et al., amhara@ipc.shizuoka.ac.jp

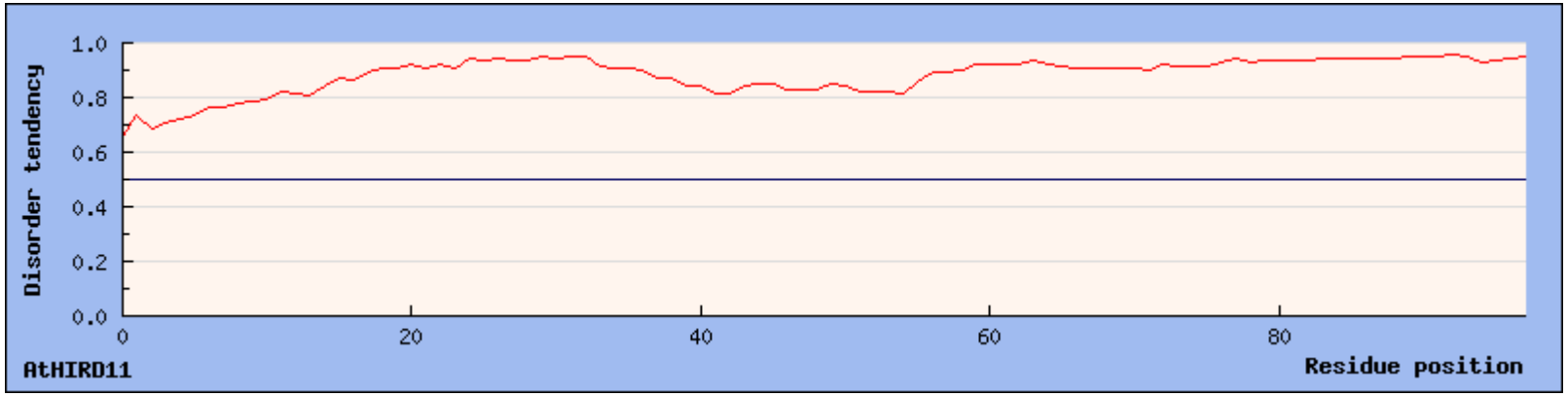

MAGLINKIGDALHIGGGNKEGEHKKEEEHKKHVDEHKSGEHKEGIVDKIKDKIHGGEGKSHDGEGKSHDGEKK
KKKDKKEKKHHDDGHHSSSSDSDSD

Supplementary Fig. S3. Prediction of disorder of AtHIRD11 by using IUPred (http://iupred.enzim.hu/). The result of the prediction is represented. AtHIRD11 shows a high disorder tendency through the sequence. The amino acid sequence of AtHIRD11 is exhibited.

Biochemical characterization of the Arabidopsis KS-type dehydrin protein, whose gene expression is constitutively abundant rather than stress dependent. Hara et al., amhara@ipc.shizuoka.ac.jp

a

```
  1: MAGLINKIGDALHIGGGNKEGEHKKEEEHKKHVDEHKSGEHKEGIVDKIK :50
 51: DKIHGGEGKSHDGEGKSHDGEKKKKKDKKEKKHHDDGHHSSSSDSDSD  :98
```

b

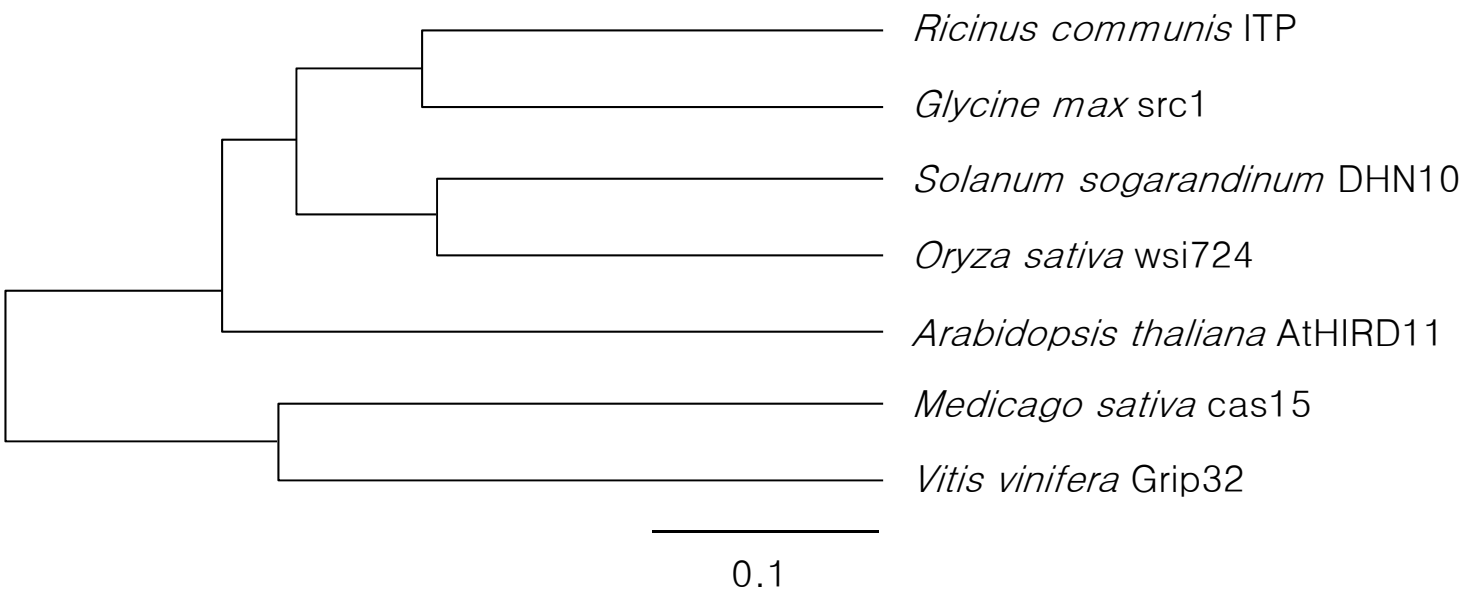

Fig. 1 Hara et al.

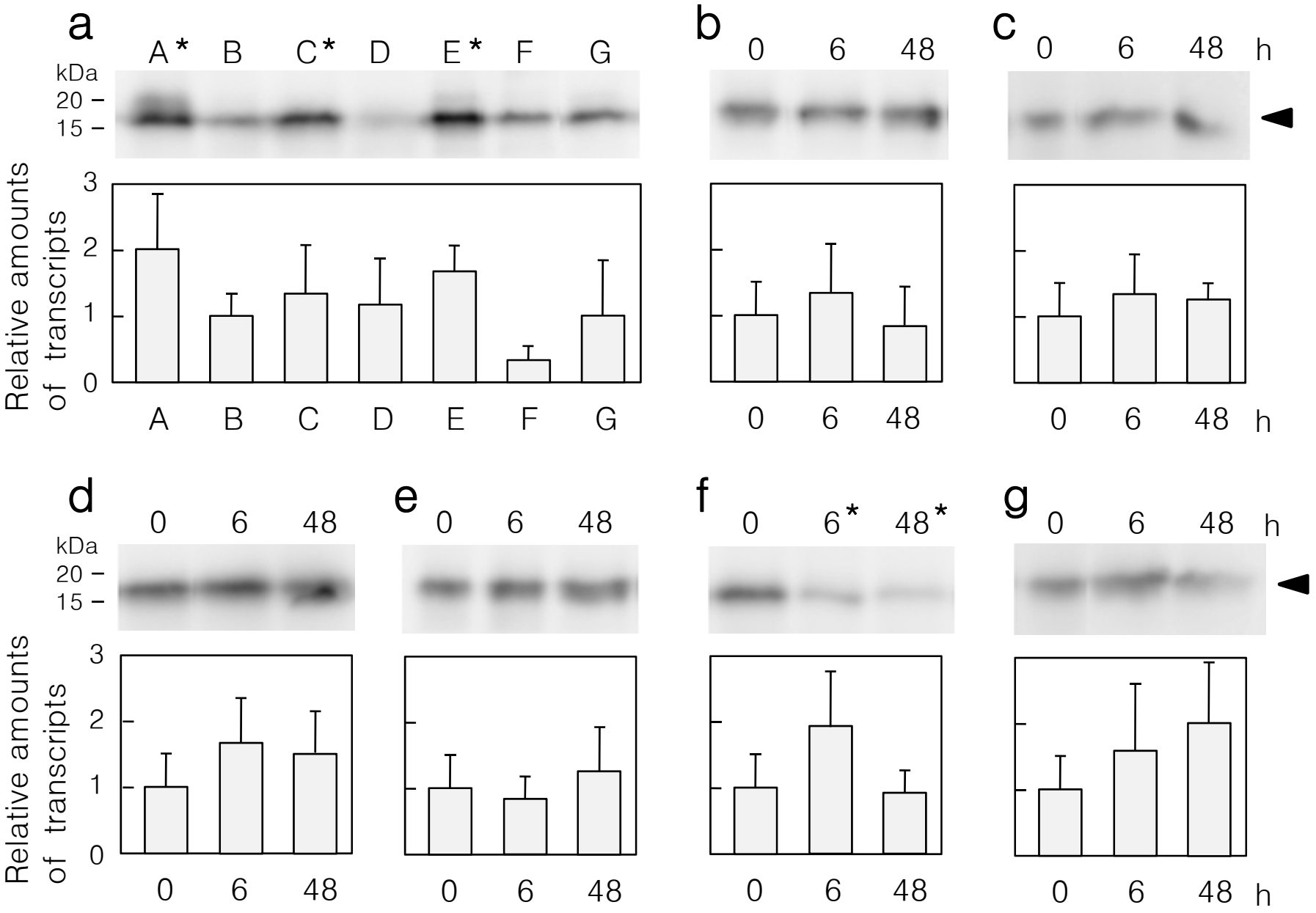

Fig. 2 Hara et al.

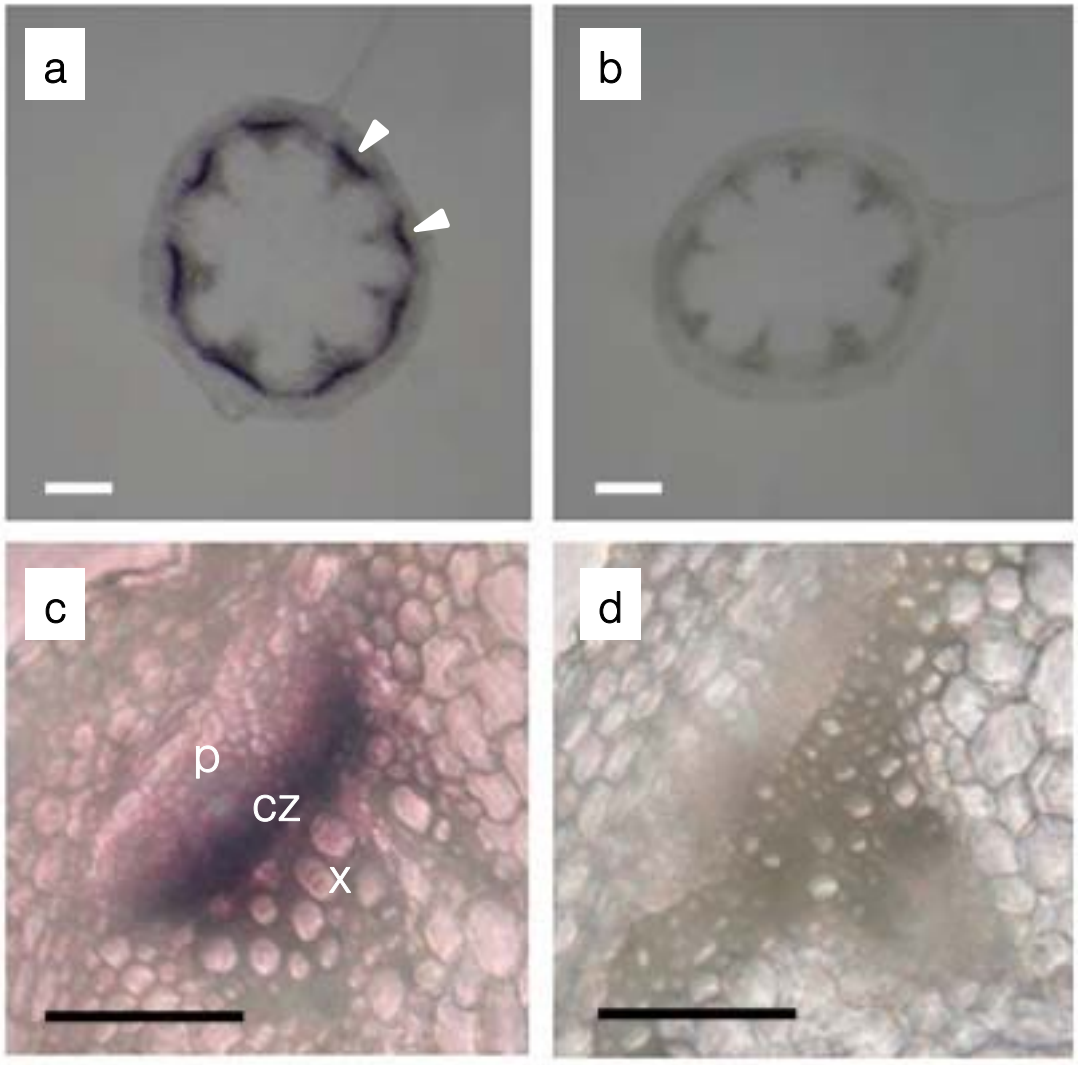

Fig. 3 Hara et al.

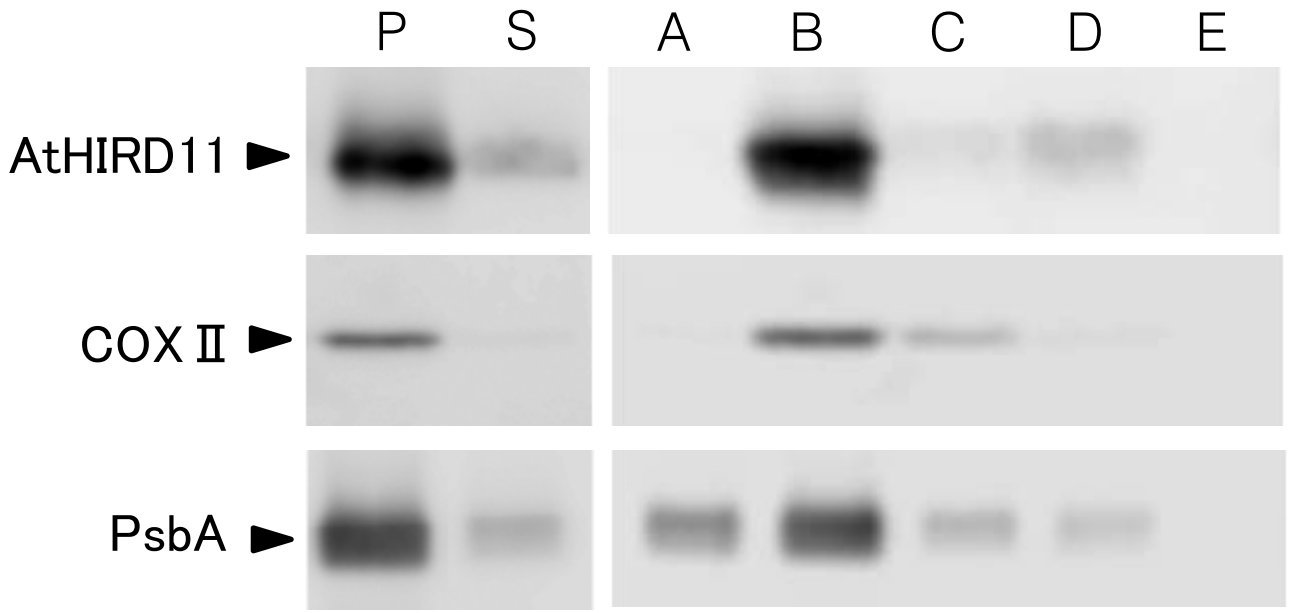

Fig. 4 Hara et al.

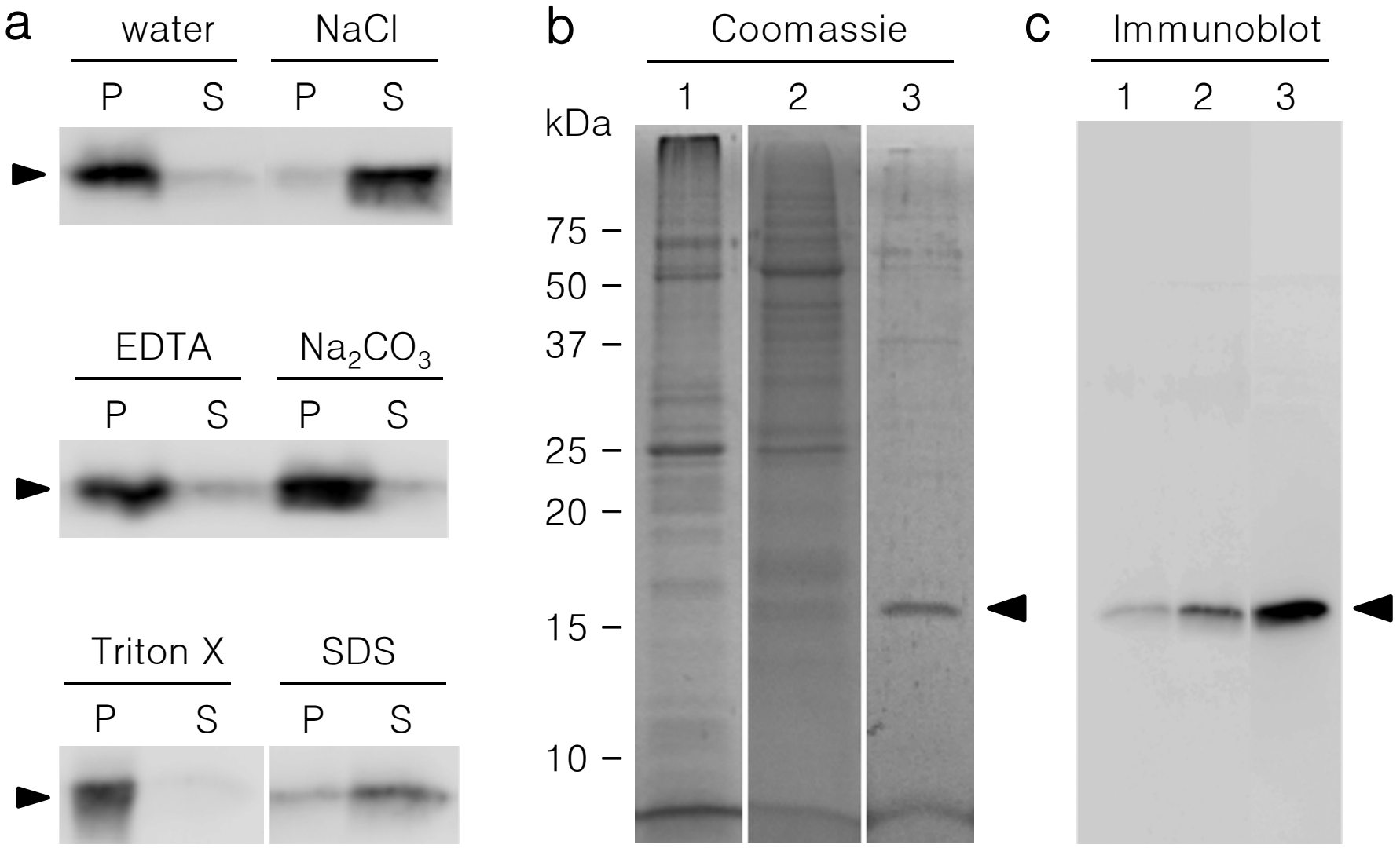

Fig. 5 Hara et al.

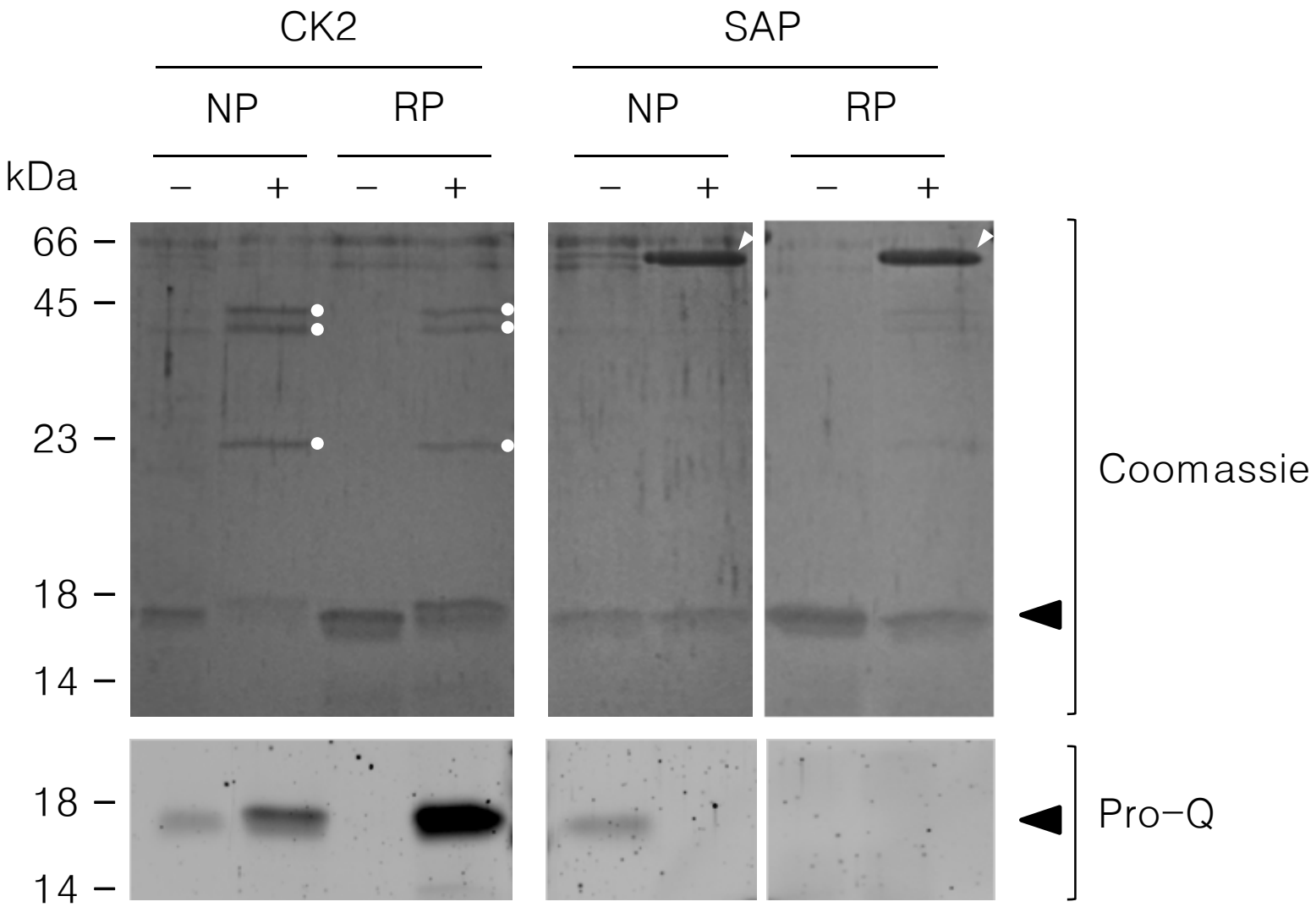

Fig. 6 Hara et al.

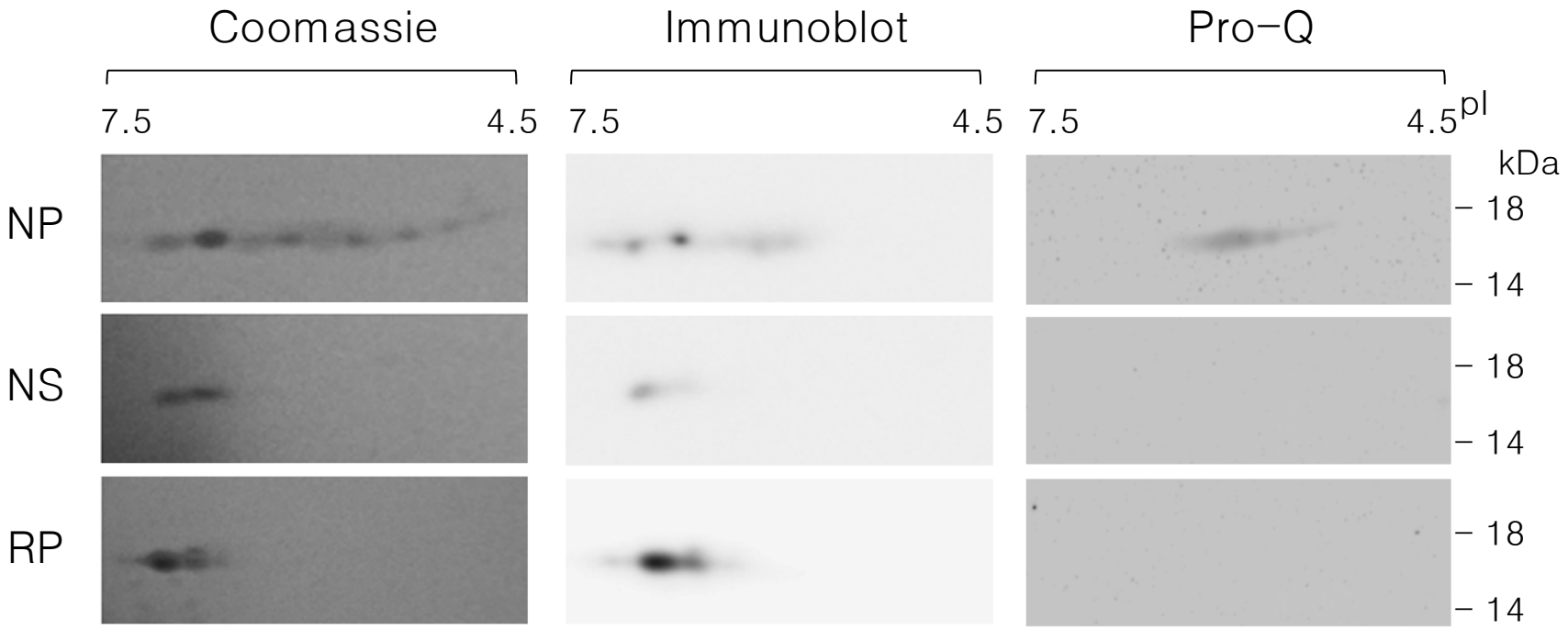

Fig. 7 Hara et al.

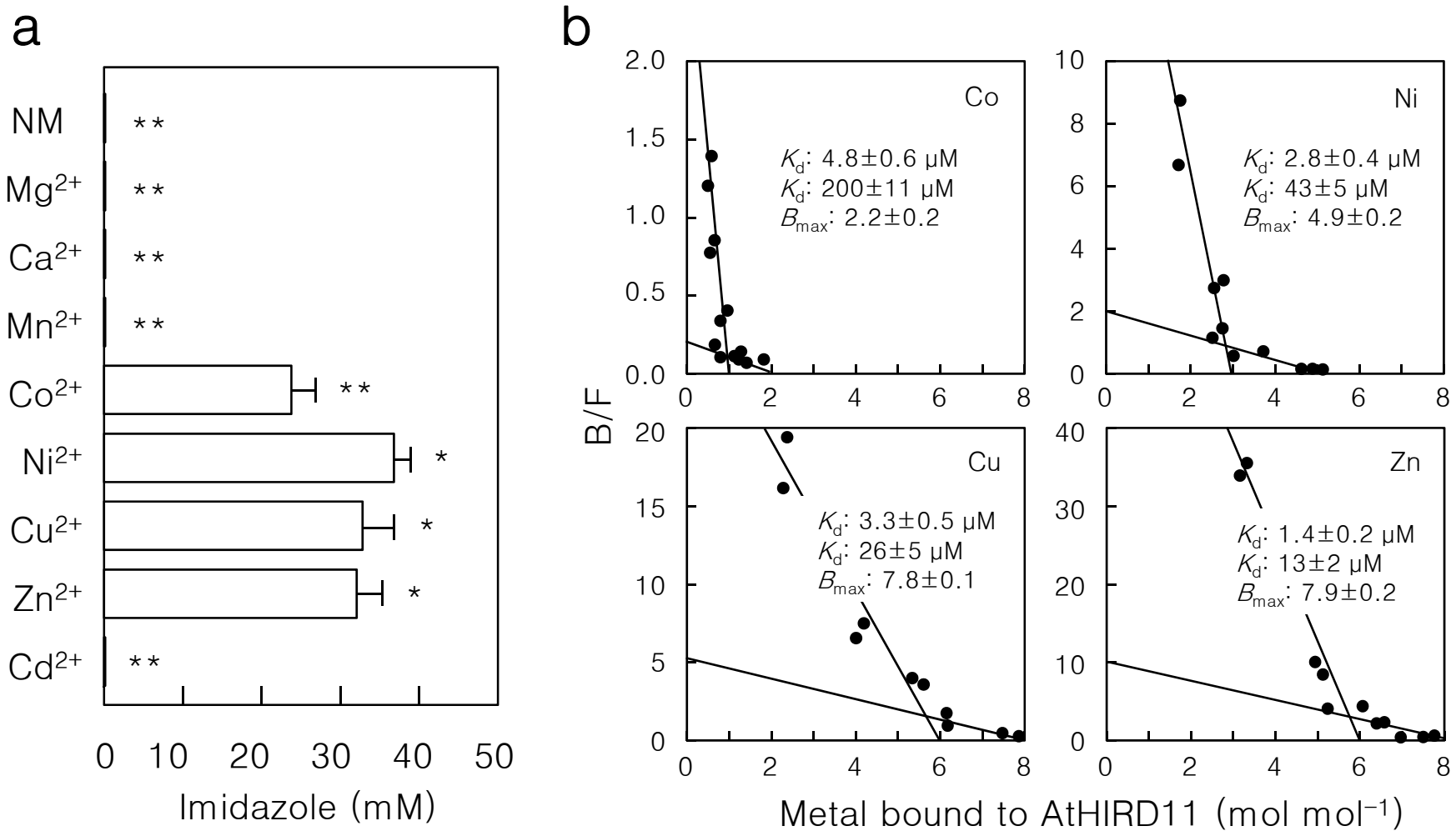

Fig. 8 Hara et al.

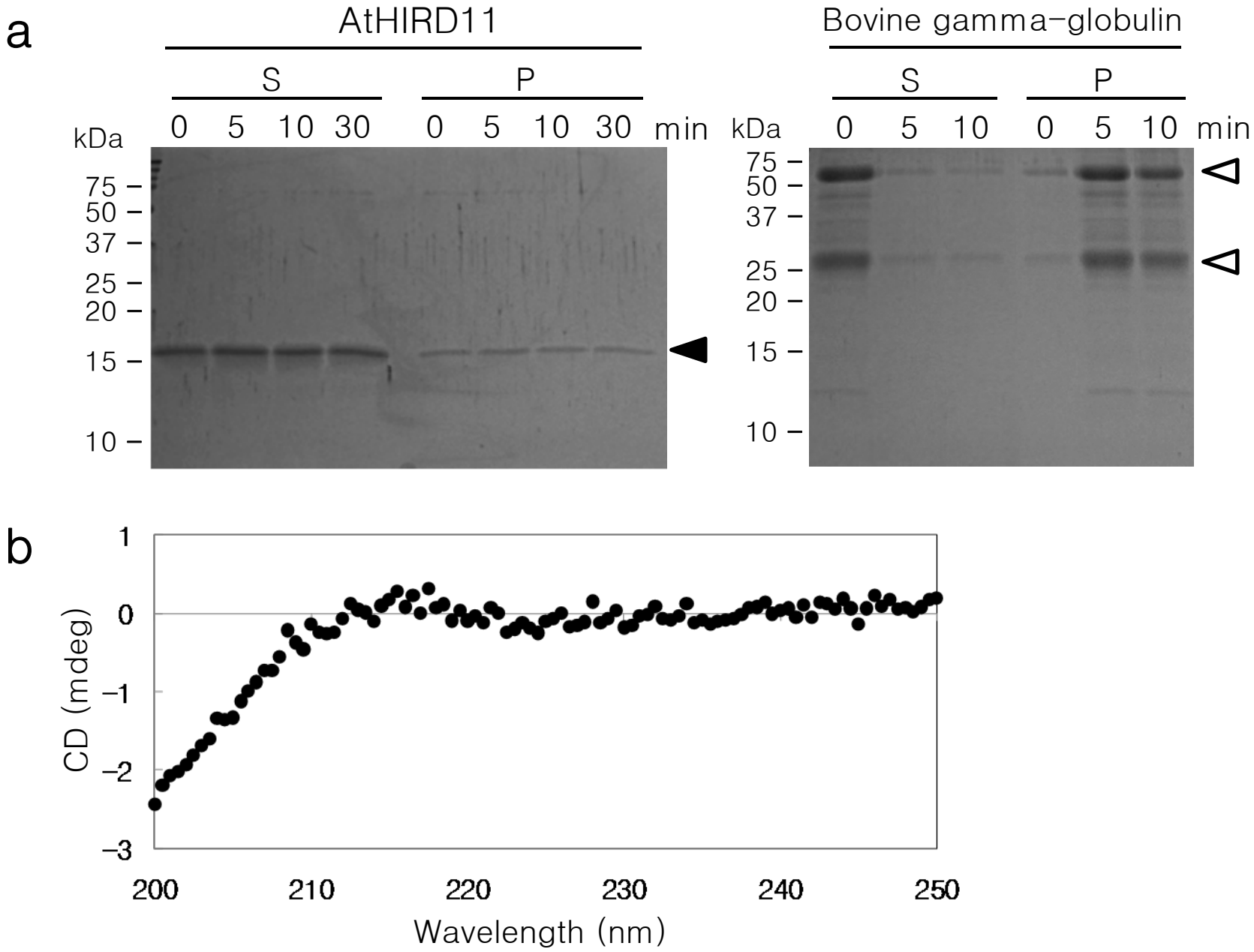

Fig. 9 Hara et al.